

Fabricating microgrooves with varied cross-sections by electrodischarge machining

Jiwang Yan · Takuya Kaneko · Kazunori Uchida · Nobuhito Yoshihara · Tsunemoto Kuriyagawa

Received: 23 September 2009 / Accepted: 1 February 2010 / Published online: 25 February 2010
© Springer-Verlag London Limited 2010

Abstract A two-step electrodischarge machining method was proposed for fabricating microgrooves with varied cross-sections on hard materials. Firstly, tungsten tool electrodes were shaped by wire electrodischarge grinding, and then the resulting tool electrodes were used to electrodischarge machine microgrooves on stainless steel. Preliminary experimental results showed that, in the first step, a sharp tool electrode with surface roughness of 0.3 μmRa could be achieved, and the surface roughness of the resulting groove was 0.16 μmRa in the second step. Voltage strongly affects the machining speed. A high voltage (>70 V) was preferable for improving the material removal rate. However, significant tool wear took place when using a high condenser capacitance at high voltages. To suppress tool wear, a high voltage and a small capacitance should be used. As test pieces, microgrooves having rectangular, triangular, circular and semi-closed cross-sections were fabricated.

Keywords Microgroove · Microchannel · Structured surface · Electrodischarge machining · EDM · Micromachining · Microfabrication

1 Introduction

In recent years, the demands for micromechanical, optical, and optoelectronic parts are increasing rapidly. These microparts not only enable the miniaturization of industrial and household-use products, but also provide new functions and special properties for the products. For many kinds of microcomponents, microgrooves having varied depths and cross-sectional shapes are key surface structures. For example, grooves can be used as slide ways in micromechanical systems, and microchannels in biomedical and biochemical applications [1, 2]. For this reason, precision manufacturing of microgrooves has become a focused research topic. Extremely fine grooves on semiconductor materials, such as silicon, can be fabricated by photolithography [3] or dry/wet etching technologies [4]. However, to generate microgrooves on metals, ceramics and glasses, mechanical approaches or nontraditional material removal processes become necessary.

Microcutting is one of the most effective techniques for machining microgrooves on metals and single crystalline materials [5–10]. End milling [5, 6], shaping [7, 8], fly cutting [9], and diamond turning [10] are four popular microcutting methods for grooves. These microgrooving techniques have been widely used in mold manufacturing for liquid-crystal display light-guiding plates, Fresnel lenses, and diffractive optical elements, etc. Electroless-plated nickel and oxygen-free copper, which have excellent machinability, are two typical workpiece materials for microcutting. However, when cutting harder materials, such as stainless steels, hardened alloys, and ceramic materials, tool wear becomes a critical problem.

Alternative methods to fabricate microgrooves would be micro-electrodischarge machining (μ -EDM) and micro-electrochemical machining (μ -ECM). These techniques

J. Yan (✉) · T. Kaneko · K. Uchida · N. Yoshihara · T. Kuriyagawa
Department of Nanomechanics, Graduate School of Engineering,
Tohoku University,
Aoba 6-6-01, Aramaki, Aoba-ku,
Sendai 980-8579, Japan
e-mail: yanjw@pm.mech.tohoku.ac.jp

can be used for machining various kinds of materials in spite of material hardness. For example, μ -EDM and μ -ECM have been used in the fabrication of microholes [11], microdimples [12], internal microstructures [13], and microtools for cutting and grinding [6, 14–18]. Yeo and Murali recently reported μ -EDM of high aspect ratio straight grooves using foil electrodes [19, 20]. However, literature on the investigation of EDM process for microgrooves which have varied cross-sections is still very little.

In the present work, we propose a two-step μ -EDM method for fabricating microgrooves with varied cross-sections. In the first step, we use the wire electrodischarge grinding (WEDG) technique [21] to fabricate tool electrodes; in the second step, we perform μ -EDM grooving tests by using the WEDG-fabricated tool electrodes. In the second step, we rotate the tool electrodes at a high speed ($\sim 3,000$ rpm) to generate a kind of “polishing effect” between the tool electrode and the workpiece. Both of the two steps are carried out on the same EDM machine, and the shapes of both the tool electrodes and the grooves can be numerically controlled. This method enables manufacturing of complex-shaped microgrooves which cannot be achieved by other machining techniques. In this paper, we report a few preliminary experimental results which will demonstrate the fundamental process characteristics of the proposed method.

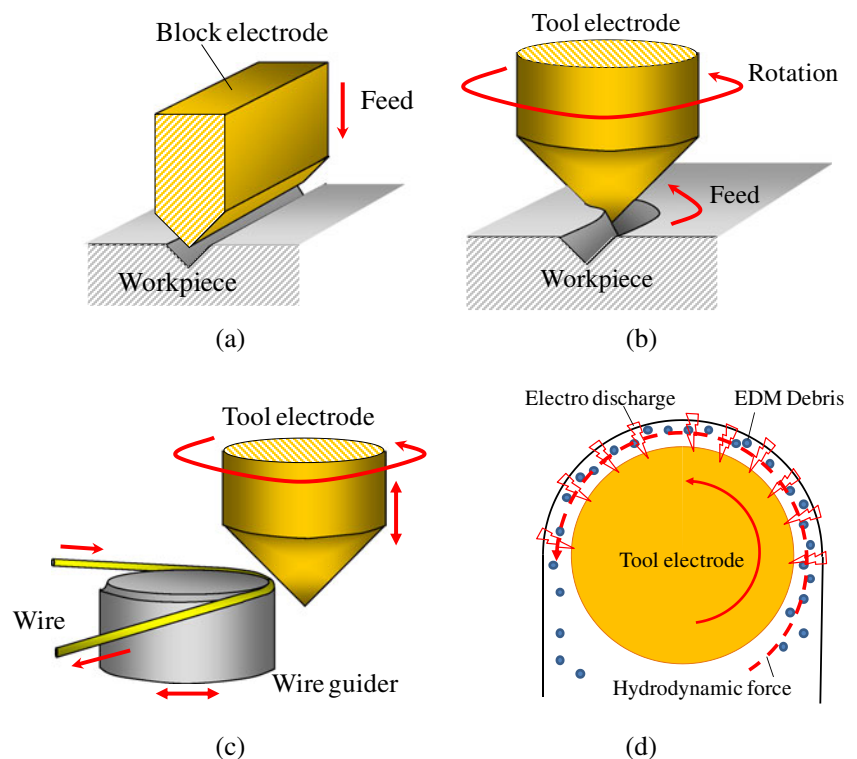
2 Experimental method and setup

2.1 Method

Two methods of EDM are usable in the fabrication of microgrooves. One is to use a shaped block electrode, as shown in Fig. 1a. When feeding the block electrode against the workpiece, electrodischarges occur between the electrode and the workpiece, and a reverse shape can be then transcribed into the workpiece. This method is suitable for fabricating straight grooves with a uniform cross-section and depth. To generate longitudinally curved microgrooves or grooves having a varied depth and cross-sectional shape, the preparation of the block electrode will be difficult.

The other method, which we proposed in this paper, is to use a high-speed rotating and moving tool electrode to generate microgrooves, as shown in Fig. 1b. This method has excellent processing flexibility and enables the manufacturing of longitudinally curved microgrooves and grooves having varied cross-sections. In this method, preparation of the microtool electrodes is an important step. We used WEDG to fabricate the tool electrodes, as schematically shown in Fig. 1c. A fine metal wire supported by a guiding wheel was used as the electrode to generate the objective shape on the tool electrode through electrodischarging. As the interference area between the wire and the tool electrode was extremely small, approach-

Fig. 1 Schematic of two EDM methods for fabricating microgrooves: **a** the conventional method using a shaped block electrode; **b** the proposed method using a rotating and three-dimensionally moving tool electrode; the tool preparation method of **b** is shown in **c**; **d** is a schematic model of polishing effect induced by high-speed rotation of the tool electrode



ing a single point, complicated shapes could be freely generated on the tool electrode by precisely controlling the relative movement between the wire and the tool electrode. Additionally, during microgrooving by rotating the tool electrode at a high speed ($\sim 3,000$ rpm), a kind of “polishing effect” is expected to take place. As schematically shown in Fig. 1d, along the gap between the tool electrode and the workpiece, debris generated by electrodischarges can be hydro-dynamically driven by the rotating tool electrode and in turn, behaves like a polishing abrasive grain. This polishing effect might assist smoothing the electrodischarge-induced microcraters on the workpiece surface.

2.2 Experimental setup

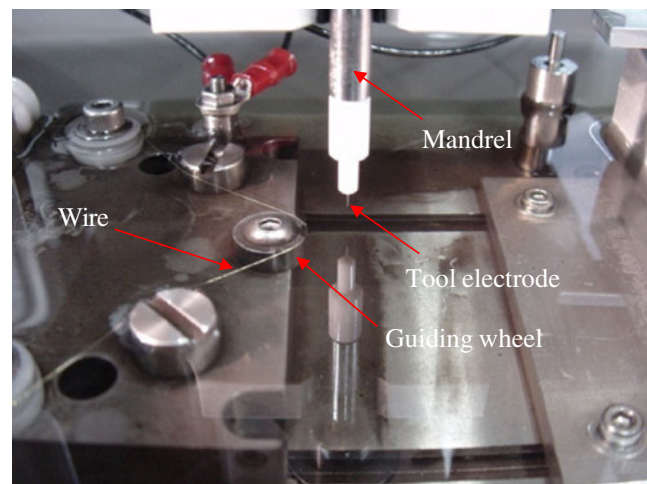
A μ -EDM machine, Panasonic MG-ED82W, produced by Matsushita Electric Industrial Co., Ltd., was used in the experiments. There are two working sections on the machine: one is a WEDG tooling section used for fabricating tool electrodes and the other is an EDM section used for microgrooving. The photographs of the two sections are shown in Fig. 2a, b, respectively. The movement of the tool electrode between the two sections can be performed by two-axis numerical control of the horizontal machine tables at a stepping resolution of $0.1 \mu\text{m}$. The tool electrode is clamped by a cylindrical mandrel which is supported by two V-type ceramic bearings on a vertically movable table. This clamping mechanism can minimize decentering errors caused by mounting and detaching of the tool electrode. The mandrel rotation is driven by a DC motor with a maximum speed of $3,000$ rpm. The conductivity between the mandrel and the electrodischarge power source is realized by steel balls.

The μ -EDM machine has an RC circuit for electrodischarge, as schematically shown in Fig. 3. There are two electrodischarging modes: one is discharging by condensers $C_1 \sim C_4$, the electrical capacities of which are $3,300$ pF, 220 pF, 100 pF, and 10 pF, respectively; the other is discharging by the stray capacitance C_0 of the circuit instead of the condensers. By using a small condenser capacitance, the RC circuit can provide very small discharge energy, which is essential for EDM of microstructures. The voltage of the power source can be changed in the range of $0 \sim 110$ V at a resolution of 1 V.

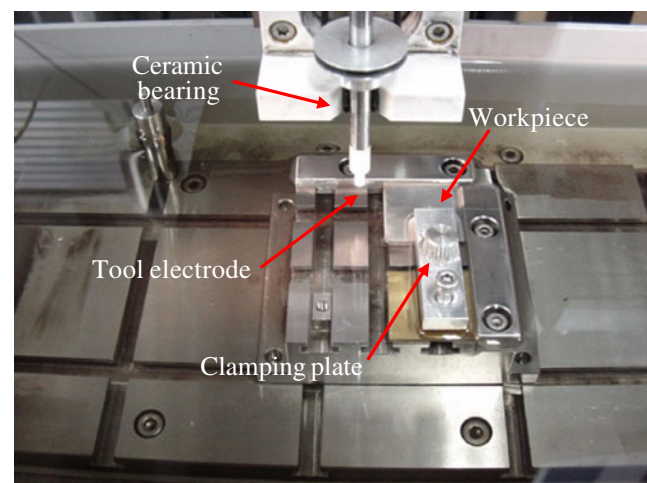
3 Fabrication of microtool electrodes

3.1 WEDG conditions

The experimental conditions for tool electrode fabrication are summarized in Table 1. A brass wire having a diameter of $100 \mu\text{m}$ was used as the negative electrode in WEDG of



(a)



(b)

Fig. 2 Photographs of the experimental setup: **a** WEDG tooling section, **b** EDM grooving section

the tool electrode. The tool electrode, namely, the positive electrode, was a $250 \mu\text{m}$ -diameter bar made of tungsten (W). Tungsten is a popular electrode material which has a high melting point and a low tool wear rate. The tool electrode was rotated by the machine spindle at a speed of

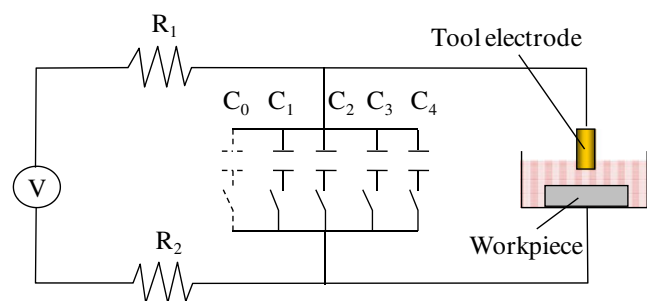


Fig. 3 Schematized RC circuit for electrodischarge

Table 1 Experimental conditions for electrode fabrication

Items	Conditions
Wire electrode (negative)	
Material	Brass
Diameter	100 μm
Feeding speed	0.5 mm/s
Tool electrode (positive)	
Material	Tungsten
Diameter	250 μm
Rotational speed	3,000 rpm
Electrodischarging media	Mitsui Space-Cut EDS oil
Voltage	70~90 V
Condenser capacitance	3,300, 220, 100, 10, and 1 pF (stray capacitance)

3,000 rpm. The Mitsui Space-Cut EDS oil was used as the electrodischarging media.

To find the optimum conditions for tool fabrication, the effects of WEDG electrodischarge energy on the finished surface roughness and geometrical error of the tool electrode were investigated. Conical tool electrodes with a 90° apex angle were fabricated under various electrodischarge energy levels by adjusting the voltage in the range of 70~90 V and the condenser capacitance from 3,300 to 10 pF. Supposing that the energy accumulated in

the RC circuit has been completely consumed by the electrodischarges, the electrodischarge energy E can be then described by

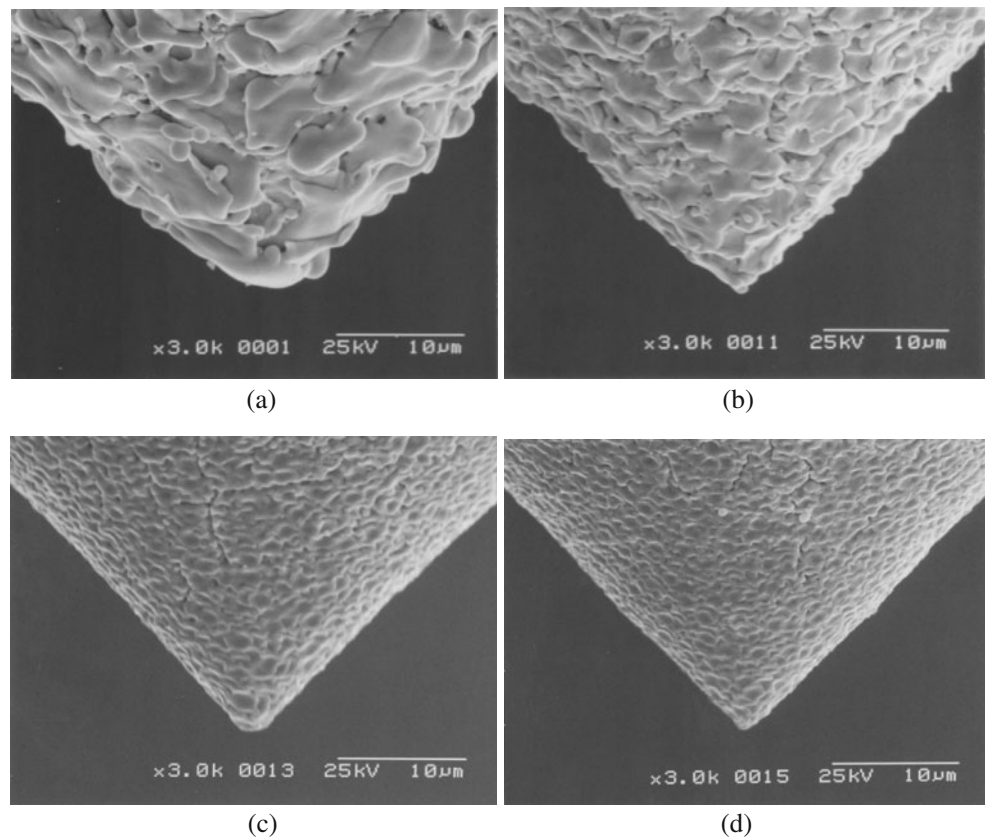
$$E = \frac{1}{2} CV^2 \quad (1)$$

Where C is the condenser capacitance and V is the voltage. As the stray capacitance of the RC circuit C_0 is very small and difficult to measure precisely, we made an approximation that $C_0=1$ pF when we use only the stray capacitance for electrodischarging.

3.2 Effects of electrodischarge energy on tool tip radius and surface roughness

First, the microtool electrodes were examined using a scanning electronic microscope (SEM). Figure 4 shows SEM micrographs of the tool electrodes fabricated under different electrodischarge energy levels. It can be seen in Fig. 4a that, at an electrodischarge energy of 13.4×10^{-6} J (voltage 90 V, condenser capacitance 3,300 pF), the tool surface is very rough and covered by a thick layer of melted and resolidified material. The size of the melted material during one electrodischarge is estimated to be ~ 10 μm . As electrodischarge energy decreases, the tool surface becomes smoother and smoother (see Fig. 4b–d). In Fig. 4d, where the electrodischarge energy is 0.00245×10^{-6} J (voltage

Fig. 4 SEM micrographs of tool electrodes fabricated under different electrodischarge energy levels: **a** 13.4×10^{-6} J (90 V, 3,300 pF), **b** 0.89×10^{-6} J (90 V, 220 pF), **c** 0.0245×10^{-6} J (70 V, 10 pF), and **d** 0.00245×10^{-6} J (70 V, 1 pF)



70 V, condenser capacitance 1 pF), the tool surface has become distinctly smooth although extremely small craters, the size of which is approximately 2 μm , can still be observed.

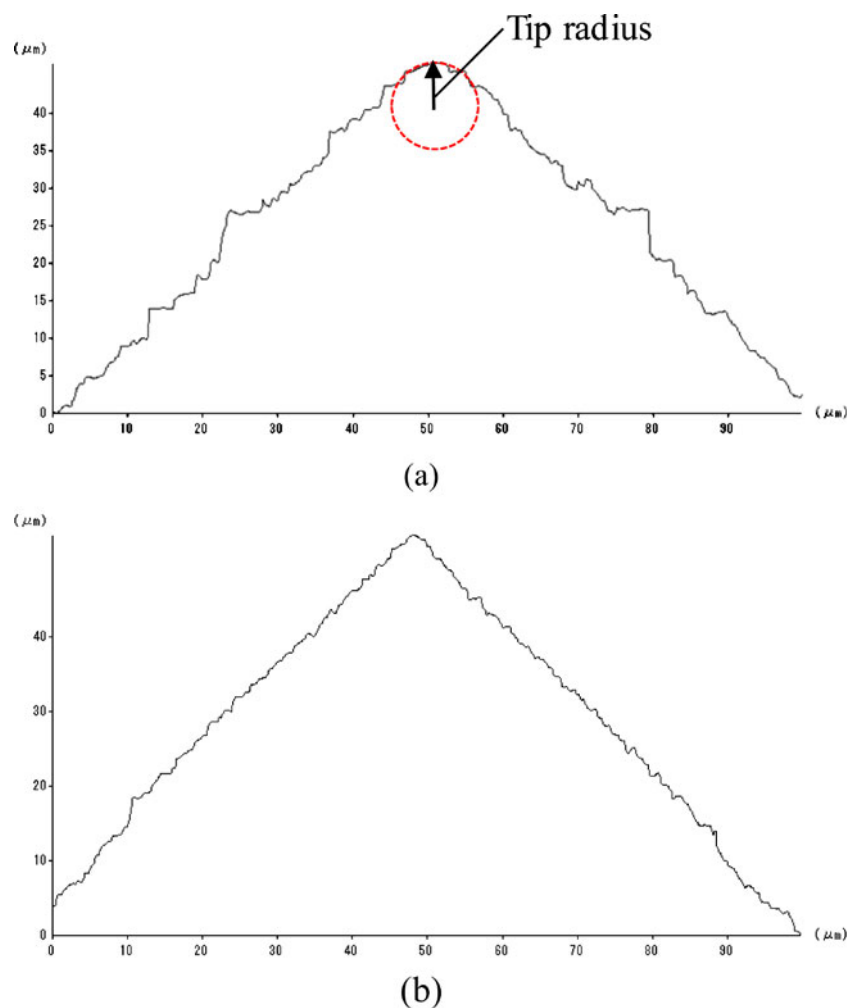
Next, the microtool electrodes were measured by a three-dimensional laser-probe profiling system, NH-3SP, produced by Mitaka Kouki Co., Ltd. Figure 5 shows two measured profiles of tool tips corresponding to the SEM micrographs in Fig. 4a, d, respectively. By fitting the tool tip with a circle using the least squares approximation, the tip radius was measured, and its change with electrodischarge energy was plotted in Fig. 6a. Five measurements were performed for each tool electrode, and the average values were indicated in the figure by red line symbols. It can be seen that as electrodischarge energy increases, the tool tip radius increases too. The smallest tip radius is approximately 1 μm while the largest one is over 6 μm . Also, the tip radius shows a remarkable divergence at high electrodischarge energy levels. Figure 6b shows the change in tool surface roughness with electrodischarge energy. The evaluation length for surface roughness was 50 μm . In

Fig. 6b, it can be seen that the surface roughness was very small ($\sim 0.3 \mu\text{mRa}$) at a low electrodischarge energy level, but increased rapidly from an electrodischarge energy of $\sim 1 \times 10^{-6}$ J. Therefore, to achieve high-precision tool electrodes with smooth surfaces, low electrodischarge energy ($< 1 \times 10^{-6}$ J) should be used.

3.3 Test pieces of microtool electrodes

Four kinds of tool electrodes were fabricated as test pieces. In the WEDG of the tool electrodes, the voltage was set to 90 V. A condenser capacitance of 3,300 pF was used for rough machining, and 10 pF was used for fine machining, respectively. Figure 7 shows SEM micrographs of the test-fabricated tool electrodes. The tool in Fig. 7a is cylindrical and having a flat end; the tool in Fig. 7b is conical (apex angle 90°); the one in Fig. 7c is spherical (end radius 30 μm), and the shape of the tool in Fig. 7d is similar to a bolt. The tool bodies were thinned from an original diameter of 250 μm to a diameter of 60 μm under rough machining conditions, and fine finishing was performed for

Fig. 5 Profiles of tool tips measured by a laser-probe three-dimensional profiling system. The profiles in **a** and **b** correspond to the SEM micrographs in Fig. 4a, d, respectively



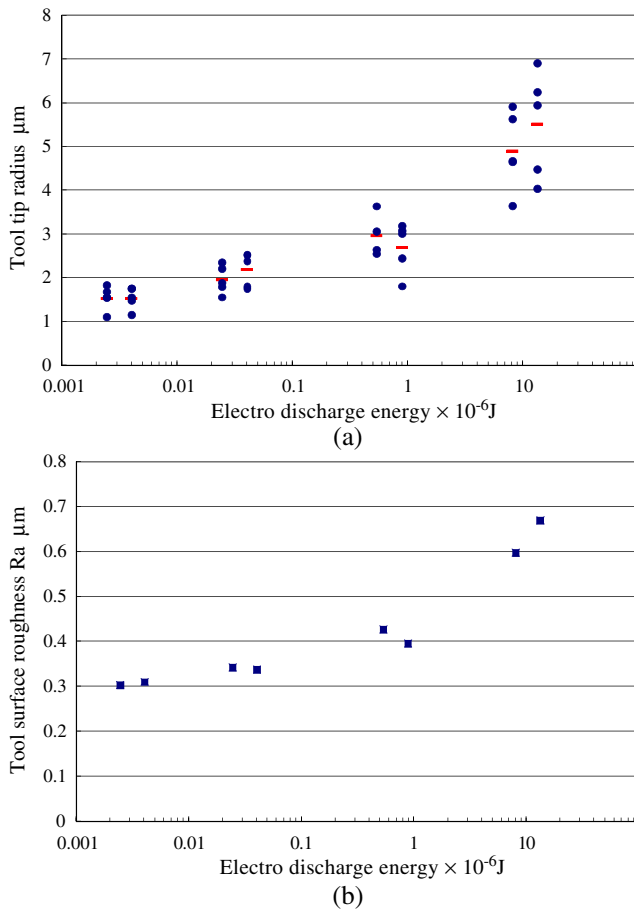


Fig. 6 Plots of **a** tool tip radius and **b** tool surface roughness against electrodischarge energy

the working surfaces of the tools. The shank of the bolt-shaped tool in Fig. 7d has a diameter of 30 μm.

4 Fabrication of microgrooves

4.1 Groove geometry and surface roughness

Using the WEDG-fabricated microtools, microgrooving tests were performed. The tools were used as the negative electrodes, and the workpiece, a chromium-alloyed martensitic stainless steel AISI 420, was used as the positive electrode. The steel has a composition of 13%Cr and 0.2%C and a hardness of 234 HV. In the experiments, the voltage between the electrodes was changed from 40 to 90 V, and the condenser capacitance was changed from 3,300 to 10 pF. Experiments were also performed by using only the stray capacitance (~1 pF) of the RC circuit instead of the condensers. The tool electrode was rotated at a speed of 3,000 rpm by the spindle. The Mitsui Space-Cut EDS oil was used as the EDM media. The experimental conditions for microgroove fabrication were summarized in Table 2.

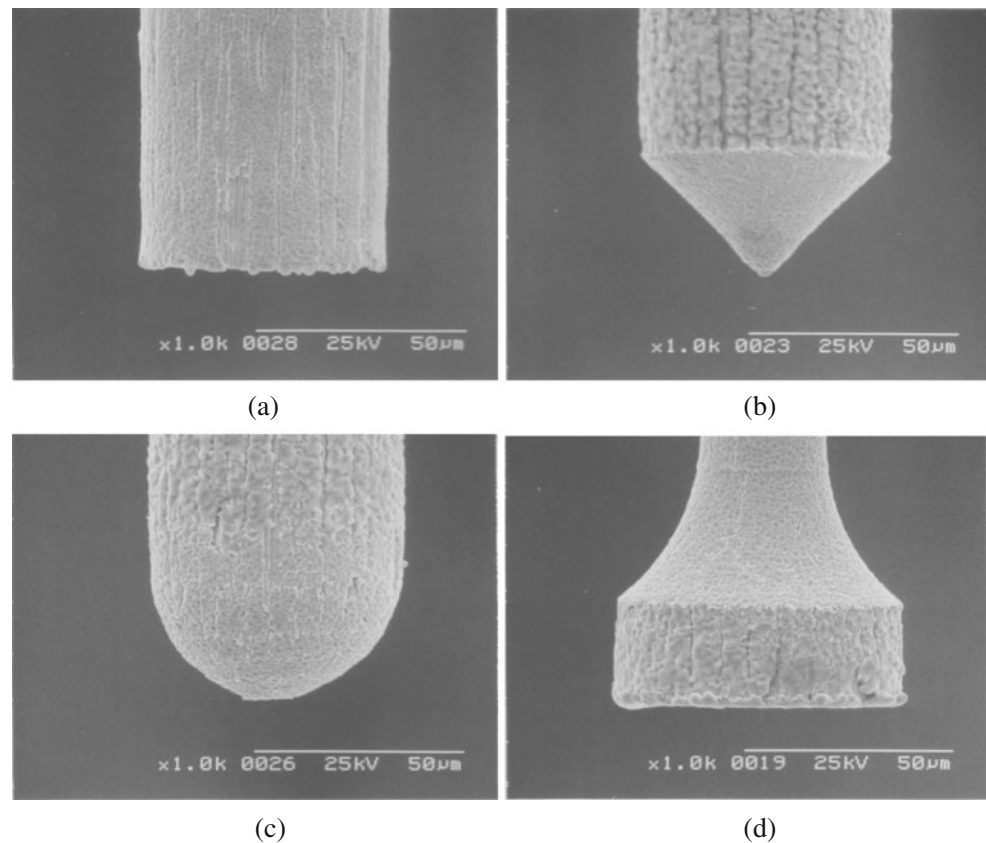
The tool electrode was approached to the workpiece at a speed 50 μm/s until the electrical current change in the RC circuit due to electrodischarge has been detected. After machining has begun, the tool feeding speed is automatically determined by the machine controller to maintain the highest material removal rate below a maximum tool feeding speed f_{\max} (in this work, $f_{\max}=2$ μm/s). If no short-cut is detected, the tool will be fed continuously at the speed f_{\max} , whereas if short-cut has been detected, the tool will be immediately drawn back slightly until the short-cut has been terminated. After the short-cut is terminated, the tool electrode will then be fed again. The details of feeding speed control strategy can be found in [22].

Figure 8 shows SEM photographs of a few micro-V-grooves fabricated using the conical tool electrodes at various electrodischarge energies. The micrographs on the right side were taken at a higher magnification than that on the left side. The grooves were 500 μm long and 30 μm deep. At a high electrodischarge energy (13.4×10^{-6} J), the surface of the microgroove was very rough and covered with a thick layer of resolidified material (Fig. 8a). Significant burrs were observed at the two sides of the groove. As the electrodischarge energy decreases, the groove surface became smoother, and the surface craters became remarkably smaller (Fig. 8b). At a low electrodischarge energy level (0.00125×10^{-6} J), the grooves surface was very smooth. The surface craters are so small that they are difficult to identify at this magnification (Fig. 8c).

Next, the microgrooves were measured by the laser-probe profiling system NH-3SP. Figure 9 is a plot of the groove bottom radius against electrodischarge energy. The radius increases gradually with electrodischarge energy below a critical value ($\sim 1 \times 10^{-6}$ J) and increases sharply beyond this value. A small radius of ~5 μm was obtained at electrodischarge energy of 0.00125×10^{-6} J [voltage 50 V and stray capacitance (~1 pF)]. As the tool electrode had an initial tip radius of 1.5 μm, it is presumable that the electrodischarge gap between the tool electrode and the workpiece was approximately 3.5 μm.

The surface roughness of the groove side walls was measured using the laser-probe profiling system. The measurement was performed along the longitudinal direction of the groove, and the evaluation length was 450 μm. Three measurements were performed for each groove by directing the laser beam to different distances (10, 20, and 30 μm) from the groove bottom. Figures 10a–c show three typical surface profiles corresponding to the microgrooves shown in Figs. 8a–c, respectively. Figure 10d is a plot of the change in average surface roughness with electrodischarge energy. The surface roughness increases with electrodischarge energy, the trend of which is similar to that in Fig. 6b. However, it is noticeable that the minimum

Fig. 7 SEM micrographs of four test-fabricated tool electrodes: **a** cylindrical, **b** conical, **c** spherical, and **d** bolt-shaped



surface roughness in Fig. 10d is $0.16 \mu\text{mRa}$, evidently lower than that in Fig. 6b ($\sim 0.3 \mu\text{mRa}$). From this result, it is presumable that at low electrodischarge energy, electrodischarge-induced microcraters were very small and could be further smoothed by the polishing effects induced by the high-speed rotation of the tool electrode. At high electrodischarge energy, however, the discharge-induced craters were too large to be smoothed by the polishing effect.

4.2 Machining speed

As mentioned in Section 4.1, a maximum value ($2 \mu\text{m/s}$) was preset to the machining speed, i.e., the tool feeding speed along the longitudinal direction of the groove, before machining. During machining, however, if shortcuts take place due to the contacts between the tool electrode and the workpiece, the tool feed will be terminated by the machine controller and the tool electrode will be slightly drawn back, leading to a loss in machining speed.

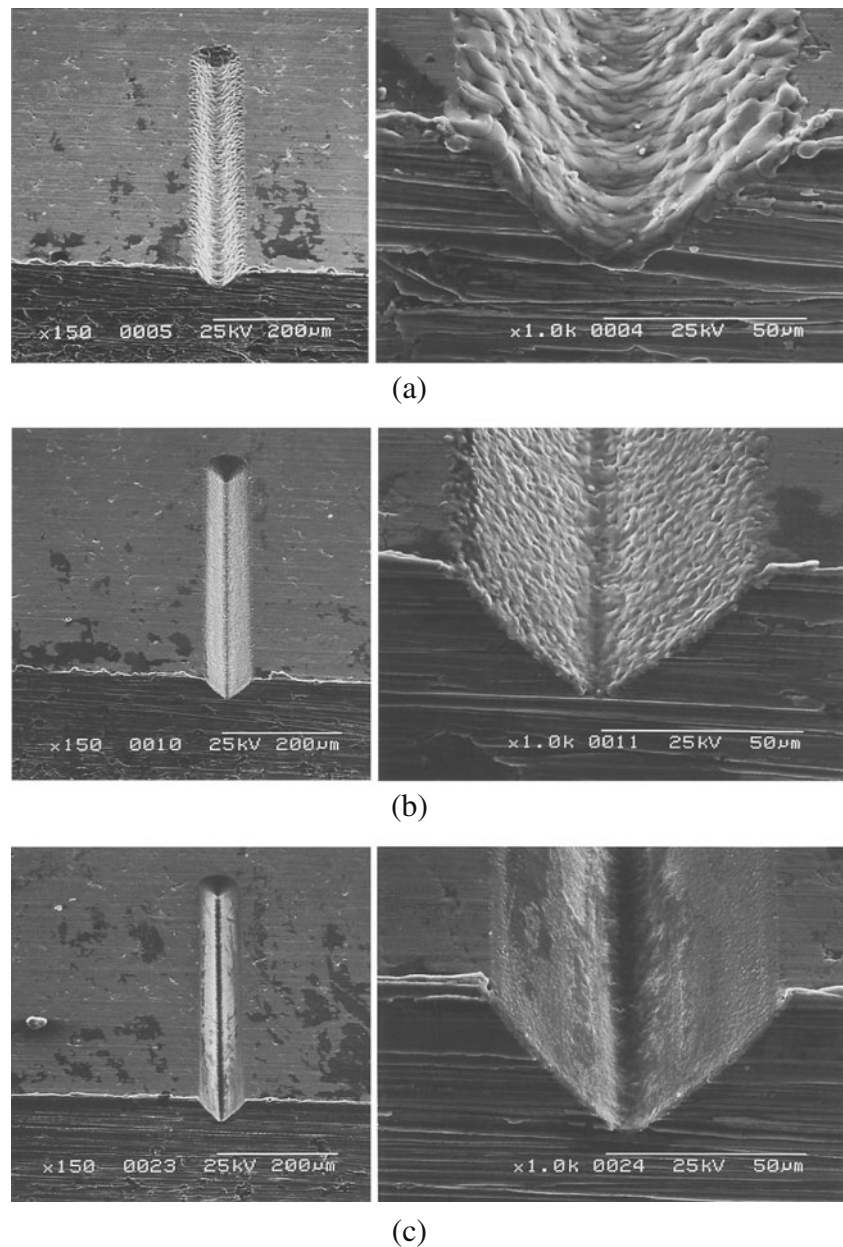
Figure 11 shows the changes in the measured machining speed during the EDM experiments. It can be seen that the voltage affects the machining speed more significantly than the condenser capacitance. At a voltage higher than 70 V , the actual machining speed approached the preset maximum machining speed, whereas at lower voltages (40 and 50 V), the machining speed dropped greatly. At a voltage of

40 V and condenser capacities of 10 and 1 pF , the machining speed approached zero. Under these conditions, the electrodischarge energy was so small that no material removal could be achieved. Therefore, it is preferable to use a high voltage ($>70 \text{ V}$) for improving the machining speed of the microgrooves.

Table 2 Experimental conditions for groove fabrication

Items	Conditions
Tool electrode (negative)	
Material	Tungsten
Shape	Cylindrical, conical, spherical, and bolt-type
Effective diameter	$30\text{--}70 \mu\text{m}$
Rotational speed	$3,000 \text{ rpm}$
Workpiece (positive)	
Material	Chromium-alloyed martensitic stainless steel AISI 420
Size	$20 \times 20 \times 2 \text{ mm}^3$
Tool feeding speed limit	$2 \mu\text{m/s}$
Electrodischarging media	Mitsui Space-Cut EDS oil
Voltage	$40\text{--}90 \text{ V}$
Condenser capacitance	$3300, 220, 100, 10,$ and 1 pF (stray capacitance)

Fig. 8 SEM photographs of micro-V-grooves fabricated using conical tool electrodes at various electrodischarge energy levels: **a** 13.4×10^{-6} J (90 V, 3,300 pF), **b** 0.539×10^{-6} J (70 V, 220 pF), and **c** 0.00125×10^{-6} J (50 V, 1 pF)



4.3 Tool wear performance

Figure 12 is an SEM micrograph of a tool electrode after use. The tool surface became smoother than that before use, and the side profiles have been slightly curved concave. The wear of tool electrodes might be attributed to two reasons: electrodischarges and polishing effects. Tool wear caused by the polishing effect increases with the distance from the tool tip. For the upper part of the tool electrode, where the circumferential speed is high, and in turn, the hydrodynamic force (see Fig. 1d) is strong, tool wear taking place due to the polishing effect is significant. Near the tool tip, however, the circumferential speed approaches zero and the polishing effect becomes insignificant. On the other

hand, the intensity of electrodischarges decreases with the distance from the tool tip. As a result, tool wear due to electrodischarge is significant around the tool tip. The tip roundness (radius $\sim 5 \mu\text{m}$) seen in Fig. 12 should be caused by the intensive electrodischarges occurring near the tool tip.

To investigate the process stability in detail, cross-sectional profiles of the grooves were measured at various machining lengths: 20, 100, 200, 300, 400, and 450 μm under various EDM conditions. Figure 13 shows changes in face angles of the V grooves with the machining length under various EDM conditions. The face angles were measured from the cross-sectional profiles of the grooves. It can be seen that for all the experimental conditions the

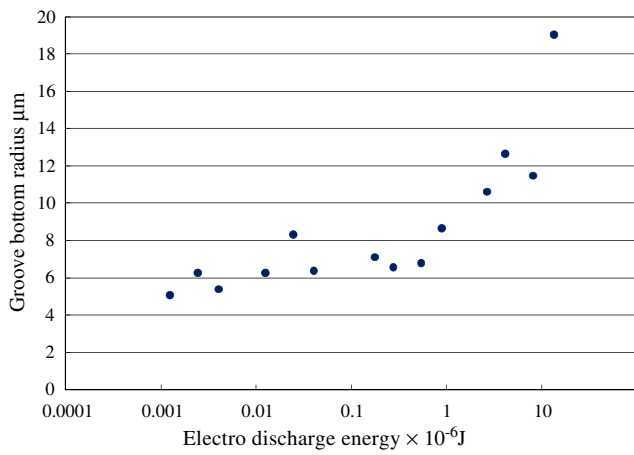
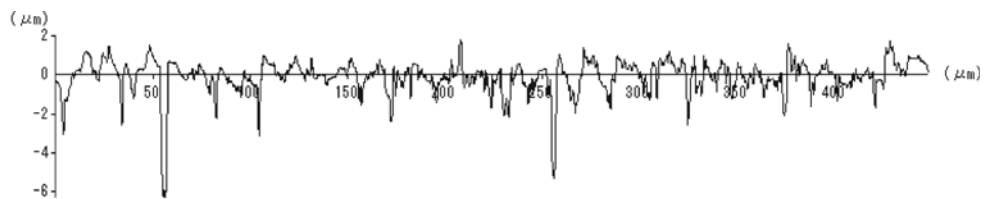
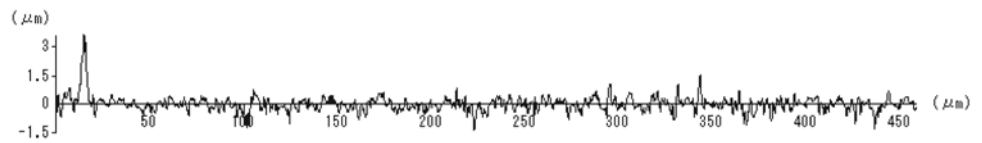


Fig. 9 Plot of groove bottom radius against electrodischarge energy

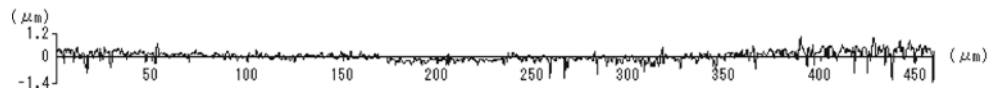
Fig. 10 Typical surface profiles of the microgrooves, **a–c** corresponding to the micrographs in Figs. 8a–c, respectively. **d** plot of the change in groove surface roughness with electrodischarge energy



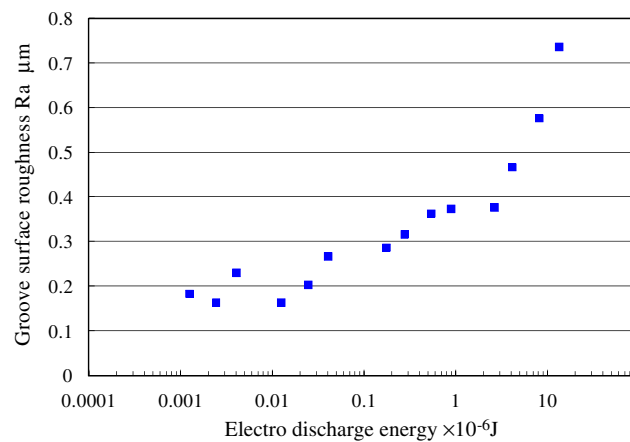
(a)



(b)



(c)



(d)

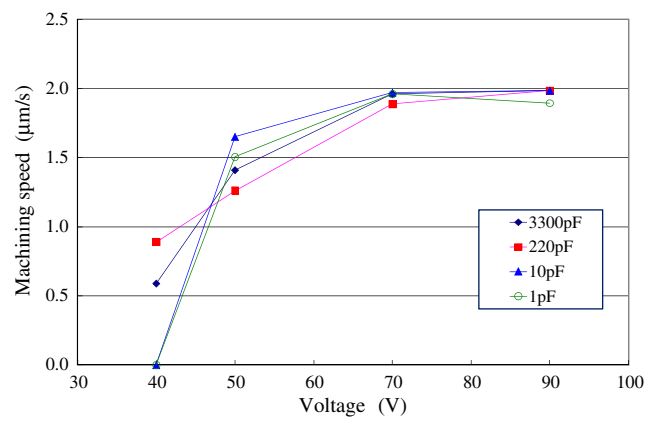


Fig. 11 Changes in the measured machining speed at various voltages and condenser capacitances

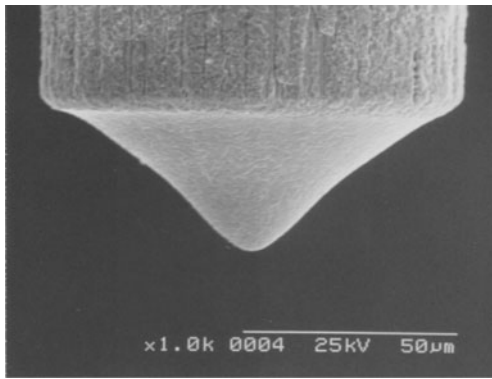


Fig. 12 SEM micrograph of a tool electrode after use, showing tool tip roundness and side profile distortion

face angles of the grooves increase with the machining length. This fact indicates that the tool tip roundness and tool tip recession due to the intensive electrodischarges occurring near the tool tip dominate the tool performance. It was note-worthy that at high voltages 90 V (Fig. 13a) and 70 V (Fig. 13b), the changes in the face angles were very small ($<10^\circ$) except for the case when using a condenser

capacitance of 3,300 pF. However, at low voltages 50 V (Fig. 13c) and 40 V (Fig. 13d), the change in the face angle was very significant ($>20^\circ$) in despite of the condenser capacitance.

After comparing the curves in Figs. 13 (a~d), we found that the most significant tool wear took place when using a high condenser capacitance (3,300 pF) at high voltages (70 and 90 V). Tool wear at a low voltage (40, 50 V) was also significant. At a low voltage, electrodischarges tended to take place much more intensively near the tool tip than that at high voltages. Therefore, it can be said that to suppress the tool wear, a high voltage and a small condenser capacitance are preferable.

4.4 Test pieces of microgrooves

Using the tool electrodes fabricated by micro-WEDG as shown in Fig. 7, four types of microgrooves, namely, rectangular (U) type, triangular (V) type, circular type, and semi-closed type, were fabricated on a stainless steel plate. The voltage and condenser capacitance used were 90 V and

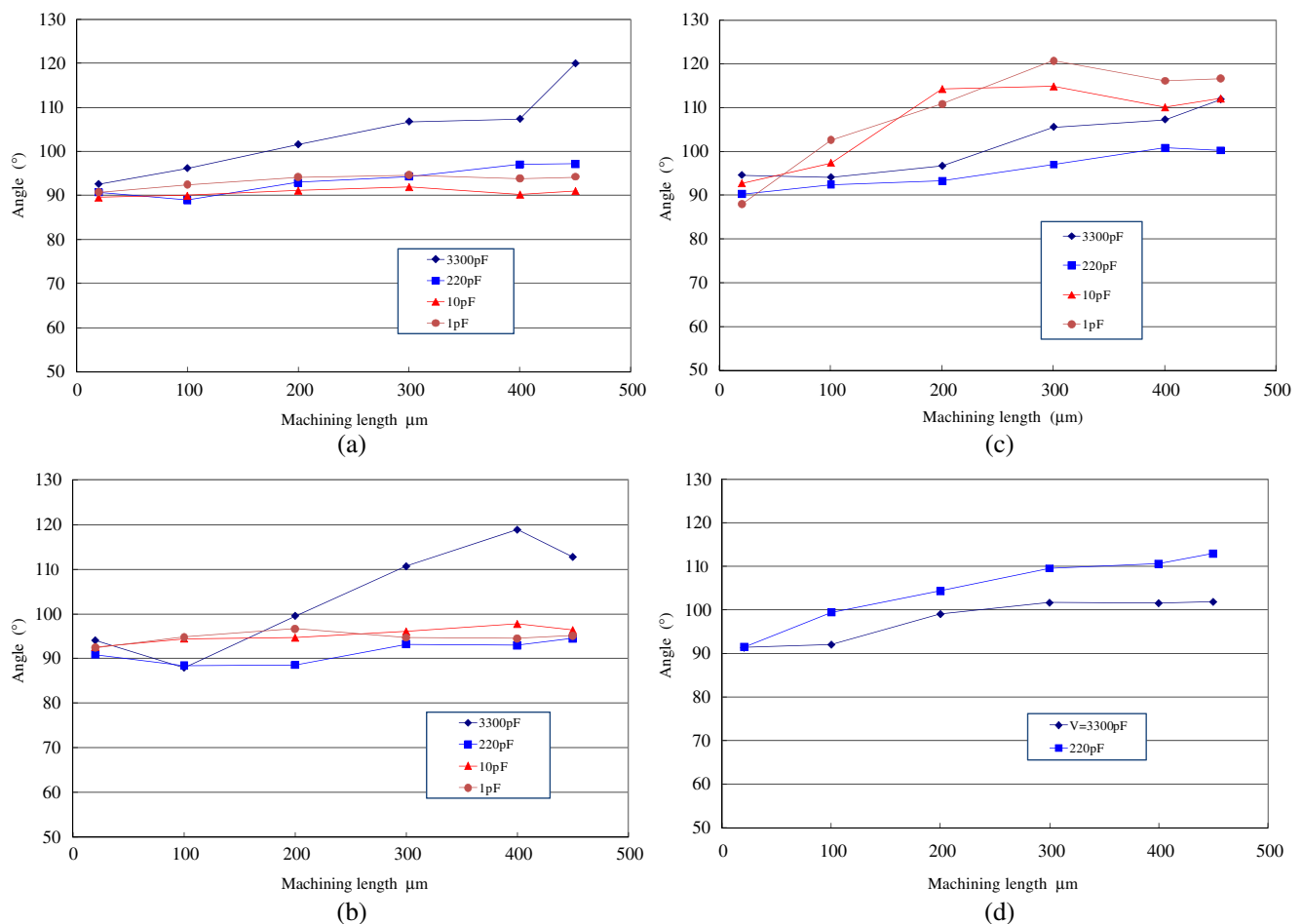


Fig. 13 Changes in face angles of V grooves with machining length under various voltages: **a** 90 V, **b** 70 V, **c** 50 V, **d** 40 V, and different condenser capacitances

10 pF, respectively. Figure 14 shows SEM micrographs of the fabricated microgrooves. The groove surfaces are very smooth, and the electrodischarge-induced microcraters are hard to identify except at the bottom of the groove shown in Fig. 14b. The surface roughness of the groove bottom is 0.16 μmRa in Fig. 14a, 0.43 μmRa in Fig. 14b, 0.21 μmRa in Fig. 14c, and 0.18 μmRa in Fig. 14d. This result demonstrated again that the high-speed rotation of the tool electrode had induced a polishing effect which assisted smoothing the craters. When fabricating a microgroove having a flat bottom (Fig. 14a,d), the circumferential speed of the tool end is high, which induces a strong polishing effect. As a result, the bottom surface becomes very smooth. When fabricating a V groove (Fig. 14b), however, the circumferential speed of the tool electrode tip approaches zero. Therefore, the polishing effect becomes very weak and cannot completely remove the microcraters induced by electrodischarges.

For simplicity, in this paper, we fabricated longitudinally straight microgrooves. By two-axis numerical control of the tool path, it is readily possible to fabricate curved ones. The microgrooves fabricated by this method might be directly usable in micromechanical systems, such as sliding ways and microassembling platforms, or in biochemical applications as microchannels.

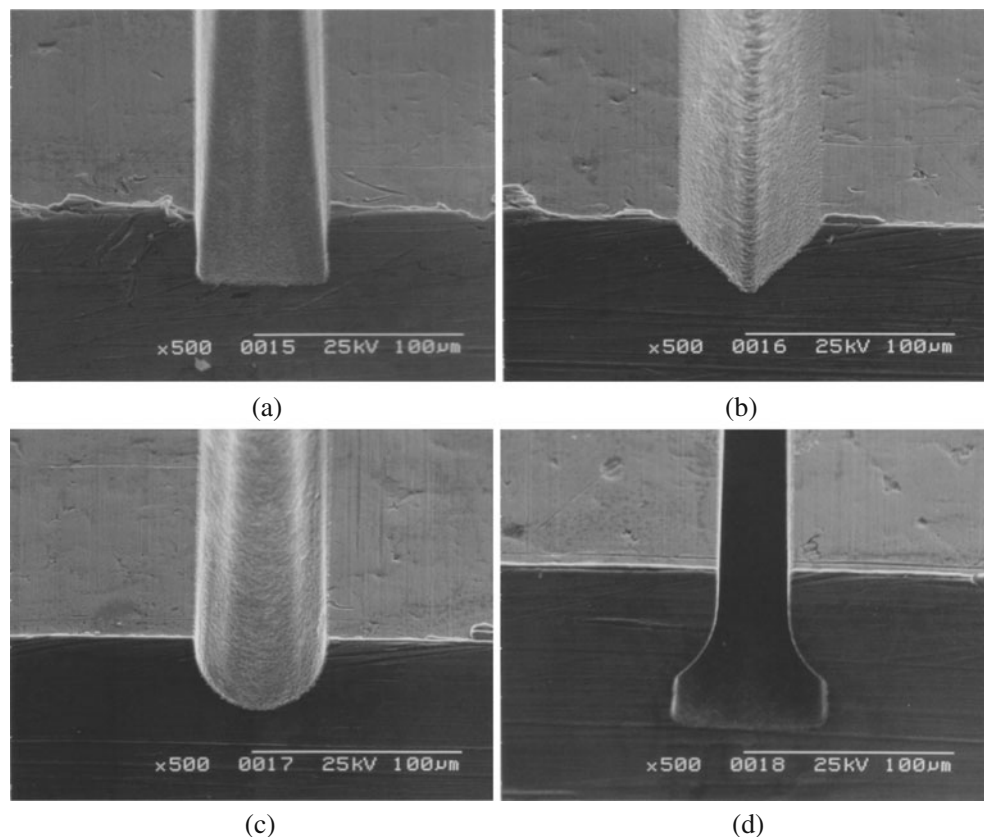
Directions of our future work include: (1) to enhance the polishing effects by rotating the tool electrodes at a higher speed and by introducing fine abrasives into the electrodischarge media; (2) to investigate the effect of tool electrode rotation speed on the machining speed, the tool wear, and the geometrical error of the fabricated grooves; (3) to explore anti-wear tool electrode materials and new media for electrodischarge to improve the service life the tool electrodes; (4) to perform on-machine measurement and compensatory resharpening of the tool electrodes. It is expected that this technique can serve high-precision flexible manufacturing of microgrooves or other microstructures on hard materials.

5 Conclusions

A two-step EDM method was proposed for fabricating microgrooves on hard materials. Fundamental machining characteristics were investigated preliminary, and the main conclusions can be summarized as follows:

1. In WEDG, as electrodischarge energy decreased, tool electrode surface roughness and tool tip radius decreased too. The smallest tool tip radius was 1.1 μm , and the

Fig. 14 SEM micrographs of the test-fabricated microgrooves having **a** rectangular, **b** triangular, **c** circular, and **d** semi-closed cross-sections



minimum surface roughness was 0.3 μmRa . In order to fabricate precise tool electrodes with smooth surfaces, low electrodischarge energy ($<1 \times 10^{-6}$ J) should be used.

2. In EDM microgrooving, as electrodischarge energy decreased, groove surface roughness and groove bottom radius both decreased. The minimum surface roughness was 0.16 μmRa , and the groove bottom radius was 5 μm at a voltage of 50 V by electrodischarging using the stray capacitance instead of condensers.
3. Voltage affected the machining speed more significantly than the condenser capacitance. It is preferable to use a high voltage (>70 V) to improve the machining speed.
4. Significant tool wear took place when using a high condenser capacitance (3,300 pF) at high voltages (70~90 V). To suppress tool wear, a high voltage and a small condenser capacitance should be used.
5. Four kinds of tungsten tool electrodes (cylindrical, conical, spherical, and bolt-shaped) were prepared, using which microgrooves having rectangular, triangular, circular, and semi-closed cross-sections were fabricated on stainless steel.

References

1. Yamaguchi Y, Ogura D, Yamashita K, Miyazaki M, Nakamura H, Maeda H (2006) A method for DNA detection in a microchannel: fluid dynamics phenomena and optimization of microchannel structure. *Talanta* 68(3):700–707
2. Noro S, Kokunai K, Shigeta M, Izawa S, Fukunishi Y (2008) Mixing enhancement and interface characteristics in a small-scale channel. *J Fluid Sci Technol* 3(8):1020–1030
3. Yao P, Schneider GJ, Prather DW (2005) Fabrication of micro-channel using planar photolithography. *Proc SPIE* 5718:73–81
4. Chan TY, Priestman GH, MacInnes JM, Allen RWK (2008) Development of a micro-channel contactor–separator for immiscible liquids. *Chem Eng Res Des* 86(1):65–74
5. Jung WC, Heo YM, Yoon GS, Shin KH, Chang SH, Kim GH, Cho MW (2007) Micro machining of injection mold inserts for fluidic channel of polymeric biochips. *Sensors* 7(8):1643–1654
6. Yan J, Uchida K, Yoshihara N, Kuriyagawa T (2009) Fabrication of micro end mills by wire EDM and some micro cutting tests. *J Micromech Microeng* 19(2):025004
7. Yan J, Oowada T, Zhou T, Kuriyagawa T (2009) Precision machining of microstructures on electroless-plated NiP surface for molding glass components. *J Mater Process Technol* 209:4802–4808
8. Kim GD, Loh BG (2007) Characteristics of chip formation in micro V-grooving using elliptical vibration cutting. *J Micromech Microeng* 17(8):1458–1466
9. Fang FZ, Liu YC (2004) On minimum exit-burr in micro cutting. *J Micromech Microeng* 14(7):984–988
10. Yan J, Maekawa K, Tamaki J, Kuriyagawa T (2005) Micro grooving on single-crystal germanium for infrared Fresnel lenses. *J Micromech Microeng* 15(10):1925–1931
11. Chen ST (2007) A high-efficiency approach for fabricating mass micro holes by batch micro EDM. *J Micromech Microeng* 17(10):1961–1970
12. Zhu D, Qu NS, Li HS, Zeng YB, Li DL, Qian SQ (2009) Electrochemical micromachining of microstructures of micro hole and dimple array. *CIRP Annals-Manufacturing Technology* 58(1):177–180
13. Jo CH, Kim BH, Chu CN (2009) Micro electrochemical machining for complex internal micro features. *CIRP Annals-Manufacturing Technology* 58(1):181–184
14. Fleischer J, Masuzawa T, Schmidt J, Knoll M (2004) New applications for micro-EDM. *J Mater Process Technol* 149:246–249
15. Chern GL, Engin Wu YJ, Cheng JC, Yao JC (2007) Study on burr formation in micro-machining using micro-tools fabricated by micro-EDM. *Precis Eng* 31(2):122–129
16. Morgan CJ, Vallance RR, Marsh ER (2004) Micro machining glass with polycrystalline diamond tools shaped by micro electro discharge machining. *J Micromech Microeng* 14:1687–1692
17. Masaki T, Kuriyagawa T, Yan J, Yoshihara N (2007) Study on shaping spherical Poly Crystalline Diamond tool by Micro-electro-Discharge Machining and micro-grinding with the tool. *Int J Surface Sci Eng* 1(4):344–359
18. Hung JC, Lien SC, Lin JK, Yuan Huang F, Yan BH (2008) Fabrication of a micro-spherical tool in EDM combined with Ni-diamond co-deposition. *J Micromech Microeng* 18(4):045010
19. Yeo SH, Murali M (2003) A new technique using foil electrodes for the electro-discharge machining of micro grooves. *J Micromech Microeng* 13(1):N1–N5
20. Murali M, Yeo SH (2004) A novel spark erosion technique for the fabrication of high aspect ratio micro-grooves. *Microsyst Technol* 10:628–632
21. Masaki T (2008) Nano-precision Electro Discharging Machining (Ph.D. thesis), Tohoku University
22. Masuzawa T, Fujino M, Kobayashi K, Suzuk T (1985) Wire electro-discharge grinding for micro-machining. *Ann CIRP* 34(1):431–434